

## Thermal analysis, structure and mechanical properties of the MC MgAl<sub>3</sub>Zn<sub>1</sub> cast alloy

**L.A. Dobrzański \***, **M. Król**, **T. Tański**

Division of Materials Processing Technology,  
Management and Computer Techniques in Materials Science,  
Institute of Engineering Materials and Biomaterials,  
Faculty of Mechanical Engineering, Silesian University of Technology,  
ul. Konarskiego 18a, 44-100 Gliwice, Poland

\* Corresponding author: E-mail address: leszek.dobrzanski@polsl.pl

Received 13.03.2010; published in revised form 01.06.2010

### Manufacturing and processing

#### ABSTRACT

**Purpose:** This work presents effect of cooling rate on the mechanical and structural properties and thermal characteristic results of MC MgAl<sub>3</sub>Zn<sub>1</sub> cast alloy.

**Design/methodology/approach:** The experiments were performed using the novel Universal Metallurgical Simulator and Analyzer Platform. Material used in this experiment is experimental magnesium alloy made as-cast.

**Findings:** The research show that the thermal analysis carried out on UMMA Technology Platform is an efficient tool for collect and calculate thermal parameters. The formation temperatures of various thermal parameters, mechanical properties (hardness and ultimate compressive strength) and grain size are shifting with an increasing cooling rate.

**Research limitations/implications:** This paper presents results for one alloy - MC MgAl<sub>3</sub>Zn<sub>1</sub> only, cooled with three different solidifications rate i.e. 0.6, 1.2 and 2.4°C/s, for assessment for the liquidus and solidus temperatures and its influence on the mechanical properties and structure.

**Practical implications:** The parameters described can be applied in metal casting industry for selecting magnesium ingot preheating temperature for semi solid processing to achieve requirements properties.

**Originality/value:** The paper contributes to better understanding and recognition an influence of different solidification condition on non-equilibrium thermal parameters of magnesium alloys.

**Keywords:** Thermal treatment; Magnesium alloys; Mechanical properties

#### Reference to this paper should be given in the following way:

L.A. Dobrzański, M. Król, T. Tański, Thermal analysis, structure and mechanical properties of the MC MgAl<sub>3</sub>Zn<sub>1</sub> cast alloy, Journal of Achievements in Materials and Manufacturing Engineering 40/2 (2010) 167-174.

## 1. Introduction

The industrial output of magnesium alloys has been rising by almost 20% per annum over recent years, which is faster than that of any other metals [1]. Magnesium alloys are stiffer and more recyclable than engineering plastics of comparable density. An equal-volume component made of magnesium is roughly 23% weight of a steel part, and in automotive weight reduction, each 100kg of weight reduction is a 5% fuel reduction [2-5]. Magnesium's physical properties are certainly influenced by the amount of added constituents. The effect of the constituent added is mostly directly pro rata to its amount. The processing and property effects of the individual alloying elements are more important in most structural applications than the physical properties. Aluminum has the most favorable effect on magnesium of any of the alloying elements. It improves strength and hardness, and it widens the freezing range, and makes the alloy easier to cast. When exceeding 6 wt%, the alloy becomes heat treatable, but commercial alloys rarely exceed 10 wt% aluminum. Zinc is next to aluminum in effectiveness, as an alloying ingredient in magnesium. It is often used in combination with aluminum to produce improvement in room-temperature strength; however, it increases hot shortness when added in amounts greater than 1 wt% to magnesium alloys containing 7-10 wt% aluminum. Zinc is also used in combination with zirconium, rare earths, or thorium to produce precipitation-hardenable magnesium alloys having good strength. Zinc also helps overcome the harmful corrosive effect of iron and nickel impurities that might be present in the magnesium alloy. Manganese does not affect tensile strength considerably, yet it slightly increases the yield strength. Its most important function is to improve saltwater resistance of Mg-Al and Mg-Al-Zn alloys by removing iron and other heavy-metal elements into relatively harmless intermetallic compounds, some of which separate out during melting. The amount of manganese that can be added is limited by its relatively low solubility in magnesium. Commercial alloys containing manganese rarely contain over 1.5 wt%, and in the presence of aluminum, the solid solubility of manganese is reduced to about 0.3 wt% [6-10].

It is well known that the cooling rate (solidification process) has a great influence on the microstructure and the mechanical properties of alloys. Even though, this effect is more pronounced when casting is the final product, wrought products can also be affected by the as-cast structure. In wrought alloys, the solidification structure and the related defects, once created, are difficult to eliminate and influence the deformation structures. Therefore, control of the solidification process often becomes vital in product quality [11]. Grain size measurements are the most common methods used to study solidification structures. An increase in solidification rate results in a reduction in grain size and an improvement in mechanical properties. Ductility and tensile strength are the properties that are influenced the most by cooling rate. AZ31 alloy is the most common commercial magnesium wrought alloy. Mg wrought alloys have in general limited formability due to hexagonal close-packed structure

and exhibit preferred orientation (texture). Recent interest in twin-roll-cast AZ31 has led to investigations on the possible links between the cast structure of AZ31 and the down-stream performance of the sheet. It is postulated that solidification structure may exert an influence on the formability and mechanical properties of alloy. The influence of the solidification conditions on the microstructure of AZ31 has not been studied in a systematic manner [12-15]. The objective of this study is to investigate the effect of cooling rate on the cast thermal parameters, microstructure and mechanical properties of MC MgAl3Zn1 cast alloy.

## 2. Experimental procedure

### 2.1. Material

The experiments have been carried out on MC MgAl3Zn1 magnesium alloys in as-cast made in cooperation with the Faculty of Metallurgy and Materials Engineering of the Technical University of Ostrava and the CKD Motory plant, Hradec Kralove in the Czech Republic. The chemical compositions of the investigated materials are given in Table 1. A casting cycle of alloys has been carried out in an induction crucible furnace using a protective salt bath Flux 12 equipped with two ceramic filters at the melting temperature of  $750\pm 10^\circ\text{C}$ , suitable for the manufactured material. In order to maintain a metallurgical purity of the melting metal, a refining with a neutral gas with the industrial name of *Emgesalem Flux 12* has been carried out. To improve the quality of a metal surface a protective layer *Alkon M62* has been applied. The material has been cast in dies with betonite binder because of its excellent sorption properties and shaped into plates of 250x150x25. The cast alloys have been heated in an electrical vacuum furnace *Classic 0816 Vak* in a protective argon atmosphere.

Table 1.

Average chemical composition (wt%) of the MC MgAl3Zn1 alloy

Al	Zn	Mn	Cu	Si	Fe
2.706	0.21	0.1	0.0018	0.032	0.005

### 2.2. Test sample

The experiments were performed using a pre-machined cylindrical test sample with a diameter of  $\phi=18\text{mm}$  and length of  $l=20\text{mm}$  taken from the ingot (Fig. 1). In order to assure high repeatability and reproducibility of the thermal data, the test sample mass was 9.1g within a very closely controlled range of  $\pm 0,1\text{g}$ . Each sample had a predrilled hole to accommodate a supersensitive K type thermocouple (with extra low thermal time constants) positioned at the center of the test sample to collect the thermal data and control the processing temperatures.

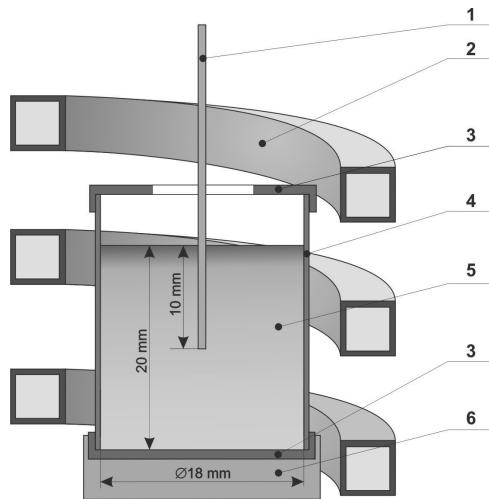


Fig. 1. Schematic of the UMSA Thermal Analysis Platform experimental set-up: 1 - low thermal mass thermocouple, 2 - heating and cooling coil, 3 - thermal insulation, 4 - steel foil, 5 - test sample, 6 - ceramic base

### 2.3. Thermal analysis

The thermal analysis during melting and solidification cycles was carried out using the Universal Metallurgical Simulator and Analyzer (UMSA) (Fig. 2) [16]. The melting and solidification experiments for the magnesium alloy were carried out using Argon as cover gas. The data for Thermal Analysis (TA) was collected using a high-speed National Instruments data acquisition system linked to a personal computer. Each TA trial was repeated three times to stabilize a process.

The TA signal in the form of heating and cooling curves was recorded during the melting and solidification cycles. The temperature vs. time and first derivative vs. temperature as well as fraction solid vs. temperature were calculated and plotted. The cooling rates for these experiments were determined using the following formula:

$$CR = \frac{T_{liq} - T_{sol}}{t_{sol} - t_{liq}} \left[ \frac{^{\circ}C}{s} \right] \quad (1)$$

were  $T_{liq}$  and  $T_{sol}$  are the liquidus and solidus temperatures ( $^{\circ}C$ ), respectively, and  $t_{liq}$  and  $t_{sol}$  the times from the cooling curve that correspond to liquidus and solidus temperatures, respectively.

The procedure comprised of the following steps. First, the test sample was heated to  $700 \pm 2^{\circ}C$  and isothermally kept at this temperature for a period of 90s in order to stabilize the melt conditions. Next, the test sample was solidified at cooling rate of approximately  $0.6^{\circ}C/s$ , that was equivalent to the solidification process under natural cooling conditions. To achieve an intentional cooling rate:

- $0.6^{\circ}C/s$  sample was cooled without forced air,
- $1.2^{\circ}C/s$  sample was cooled in airflow 30 l/min,
- $2.4^{\circ}C/s$  sample was cooled in airflow 125 l/min.

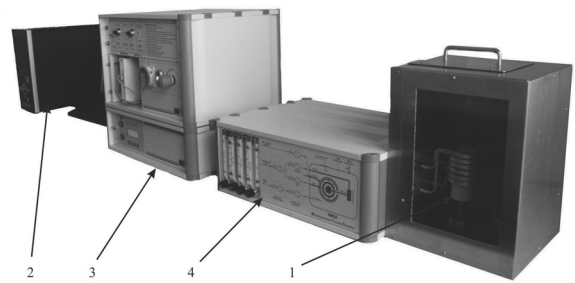


Fig. 2. UMSA apparatus - (1) sample chamber, (2) supervisory computer, (3) temperature control, (4) gas flow control

Table 2. Characteristic points obtained from thermal-derivative analysis

Point	Temperature	Description
1	$T_N$	Nucleation of $\alpha$ -phase (liquidus temperature)
2	$T_{Dmin}$	The $\alpha$ -Mg dendrite minimum (undercooling) temperature
3	$T_{DKP}$	Coherency point
4	$T_G$	The $\alpha$ -Mg dendrite growth temperature
5	$T_{sol}$	End of solidification (solidus temperature)

The magnesium nucleation temperature  $T_N$ ,  $T_{Dmin}$ ,  $T_{DKP}$ ,  $T_G$ , and solidus temperatures  $T_{sol}$ , where calculated using the first derivative of the cooling curve. The  $\alpha$ -Mg Dendrite Nucleation Temperature, ( $T^{\alpha DEN}_{NUC}$ ) represents the point at which primary stable dendrites start to solidify from the melt. This event is manifested by the change in the slope of the cooling curve and determined by the first derivative inflection point. The liquidus temperature signifies the beginning of the fraction solid that, at this point, is equal to zero. The  $\alpha$ -Mg Dendrite Minimum (Undercooling) Temperature, ( $T^{\alpha DEN}_{MIN}$ ) represents a state where the nucleated dendrites have grown to such an extent that the liberated latent heat of fusion balances the heat extracted from the test sample. After passing this point, the melt temperature increases to a steady state growth temperature ( $T^{\alpha DEN}_G$ ).  $T^{\alpha DEN}_{NUC}$  as the local minimum is determined by the point at which the first derivative intersects the zero line ( $dT/dt=0$ ). The time period required for heating up of the test sample to the  $T^{\alpha DEN}_G$  is called recalescence. At the start of solidification of a melt, small equiaxed crystals are developing, separate from one another. The viscosity of the melt and hence torque is very small. As the dendrites grow in size and start to impinge upon one another, a continuous solid network builds up throughout the sample volume. There is a sudden increase in the torque force needed to shear the solid network. This point is called "coherency point". The  $\alpha$ -Mg Dendrite Growth Temperature, ( $T^{\alpha DEN}_G$ ) represents the local maximum temperature of this reaction (and is also called the "steady state growth temperature). The  $T^{\alpha DEN}_G$  corresponds to the second zero point on the first derivative curve ( $dT/dt=0$ ) following the start of nucleation ( $dT/dt = 0$ ). If the first derivative curve in this region does not intersect the zero line,

$T_{MIN}^{\alpha DEN}$  the  $T_G^{\alpha DEN}$  temperatures are identical and correspond to the maximum point on the first derivative curve (Fig. 3 and Table 2).

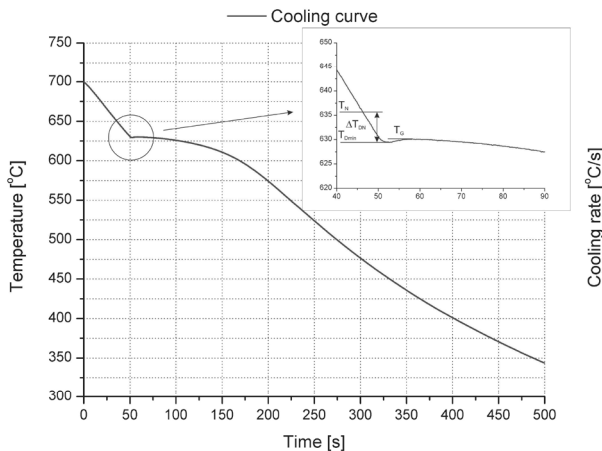


Fig. 3. Cooling curve of MC MgAl<sub>3</sub>Zn1 alloy obtained under non-equilibrium experimental condition:  $\Delta T_{DN}$  nucleation undercooling

## 2.4. Microstructure examinations

Metallographic samples were taken from a location close to the thermocouple tip. Samples were cold mounted and grounded on 240, 320, 400, 600 and 1200 grit SiC paper and then polished with 6 $\mu$ m, 3 $\mu$ m and 1 $\mu$ m diamond paste. The polished surfaces were etched with a solution of 2g oxalic acid, 100ml water, with fresh alcohol blotted repeatedly onto the surface to prevent residue deposits.

The X-ray qualitative and quantitative microanalysis and the analysis of a surface distribution of cast elements in the examined magnesium cast alloys have been made on the Opton DSM-940 scanning microscope with the Oxford EDS LINK ISIS dispersive radiation spectrometer at the accelerating voltage of 15 kV. Phase composition and crystallographic structure were determined by the X-ray diffraction method using the XPert device with a copper lamp, with 40 kV voltage. The measurement was performed by angle range of 2 $\theta$ : 30° - 120°.

## 3. Results and discussions

### 3.1. Thermal analysis results

The cooling curves recorded for MC MgAl<sub>3</sub>Zn1 alloy at various cooling rates are shown in Fig. 4. It is seen that formation temperatures of the various phases are changed when the cooling rate is increased. The shift magnitude increases with an increasing cooling rate. This shift changes the characteristic parameters of thermal analysis particularly in the liquidus region.

The cooling rate is proportional to the heat extraction from the sample during solidification. Therefore, at a low cooling rate (0.6 °C/s), the rate of heat extraction from the sample is slow and the slope of the cooling curve is small. So, it creates a wide cooling curve. But, at a high cooling rate (2.4 °C/s) the rate of heat extraction from the sample is fast, the slope of the cooling curve is steep and it makes a narrow cooling curve.

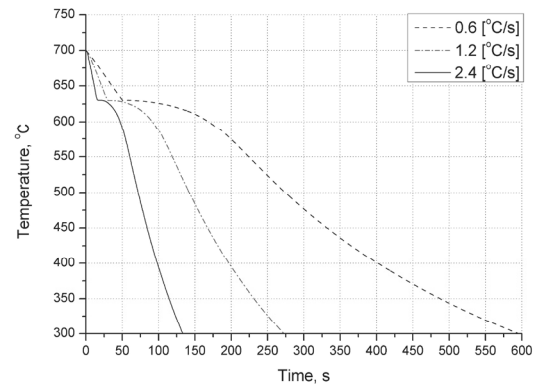


Fig. 4. Cooling curves of MC MgAl<sub>3</sub>Zn1 alloy at various cooling rates

Thermal analysis of the magnesium alloys have been presented on Figure 5. One visible temperature arrest was noted on the cooling curves. More detailed information pertaining to the alloy's thermal characteristics such as non-equilibrium liquidus, etc. were determined using the first derivative curves. The temperatures of the metallurgical reactions are presented in Table 3. Based on the cooling curve analysis, the non-equilibrium liquidus temperature of MC MgAl<sub>3</sub>Zn1 alloy that solidified at 0.6°C/s was found approximately 633.16 $\pm$ 0.85°C. At this temperature the first magnesium dendrites, most likely, nucleated from the melt. Latent heat evolved and caused the temperature of the surrounding melt to rise. This point was clearly visible as a sudden change in the first derivative curve. At 630.44°C the next change in the first derivative curve was observed and corresponded to the  $\alpha$ -Mg dendrite minimum temperature. The coherency point was observed at 630.64°C. The next point at Fig. 5 corresponded to  $\alpha$ -Mg dendrite growth temperature was observed at 630.85°C. It was found that non-equilibrium solidus temperature was approximately 508.96°C. Parameters for magnesium alloys that solidify at highest solidification rate are presents in table 3. It can be noted that the  $\alpha$ -Mg dendrite minimum temperature and coherency point wasn't observed.

Figure 6 shows the variation of the magnesium nucleation temperature as a function of cooling rate and the variation of the Mg nucleation undercooling temperature. Standard errors calculated for each measured data point have also been included in the graph. It is evidence from the plot, that the Mg nucleation temperature increase with increase cooling rate from 0.6 to 2.4°C/s, the Mg nucleation temperature increases from 633.16 $\pm$ 0.85°C to 640.32 $\pm$ 4.58°C. Increasing the cooling rate increases the heat extraction. Due to the increase the cooling rate the nucleation undercooling increase from 2.31 to

10.61°C. The phenomena of an increase in the nucleation temperature with an increase in the solidification rate depends on the mobility of the clusters of atoms in the melt. These groups of the froze atoms produces the fluctuation clusters and fluctuation embryos, which are the nucleation primers. The increase of the cooling rate with an increase amount of the nucleation primers and reduction of the recalescence temperature is well established fact.

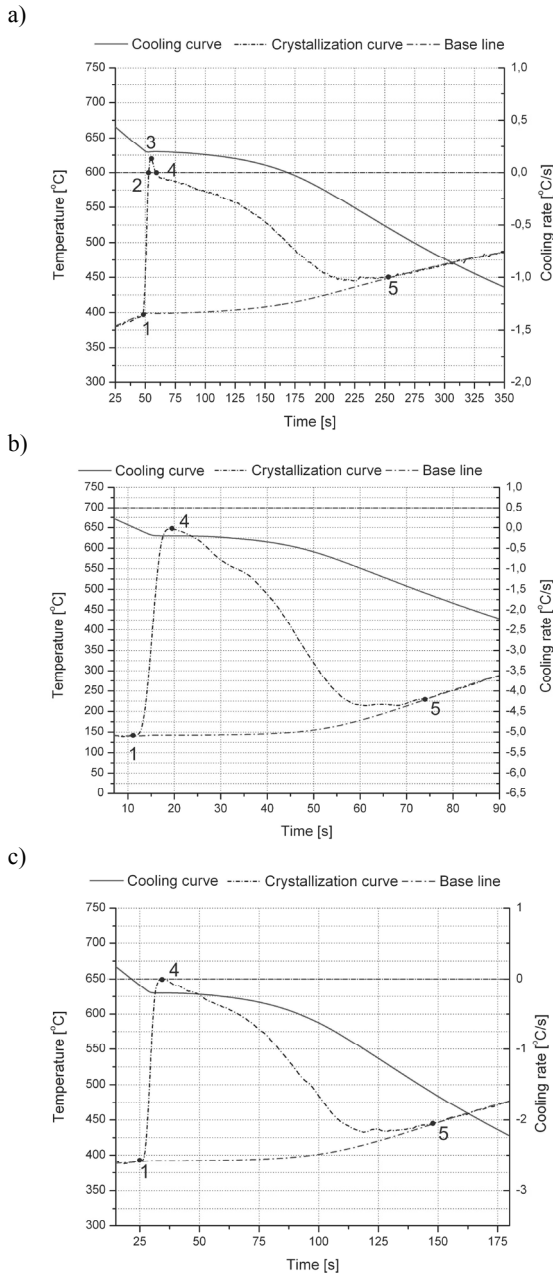


Fig. 5. Cooling, crystallization and calorimetric curves of the magnesium alloy solidified with cooling rate: a) 0.6°C/s, b) 1.2°C/s, c) 2.4°C/s.

Table 3. Non-equilibrium thermal characteristics of the MC MgAl3Zn1 alloy test samples obtained during the solidification process at 0.6°C/s, 1.2°C/s and 2.4°C/s solidification rates

Characteristic point	Solidification rate [°C/s]		
	0.6	1.2	2.4
1	633.16±0.85	635.39±1.92	640.32±4.58
2	630.44±0.94	Not observed	
3	630.64±0.89	Not observed	
4	630.85±0.86	630.42±0.76	629.71±0.64
5	508.96±12.42	502.03±7.18	492.28±5.16

Figure 7 presents an influence of cooling rate on solidus temperature. As can be seen that the cooling rate increases cause solidus temperature decreases, resulting from widening the solidification range from 124°C to 148°C.

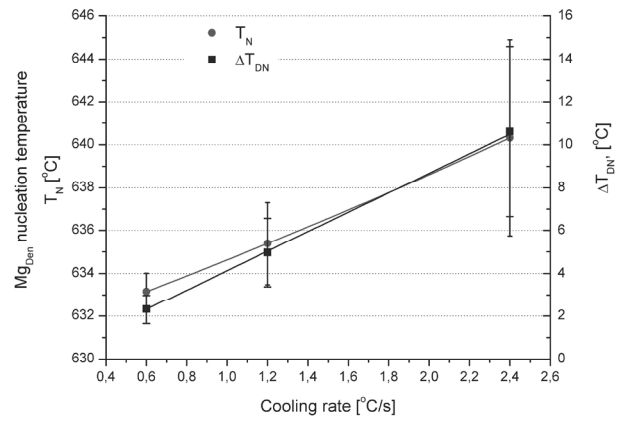


Fig. 6. Variation of the Mg nucleate temperature as a function of cooling rate and variation of the Mg nucleate undercooling temperature as a function of cooling rate

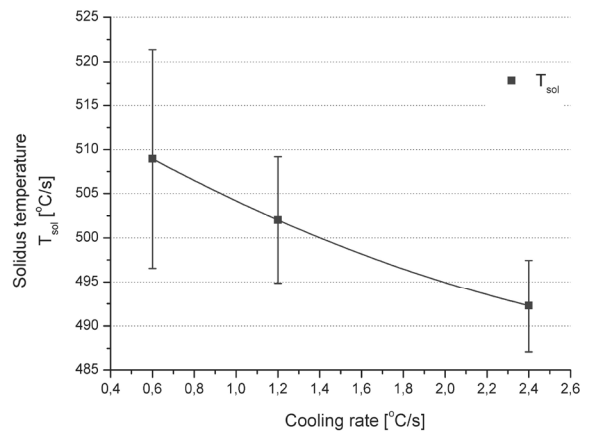


Fig. 7. Variation of the solidus temperature as a function of cooling rate.

### 3.2. Structure characteristic

According to the X-ray phase analysis, the investigated MC MgAl3Zn1 alloy cooled with solidification rate: 0.6, 1.2 and 2.4 °C/s is composed of one phase (Fig. 8.):  $\alpha$ -Mg solid solution as matrix. In the diffraction pattern of the matrix, the {011} Mg-diffraction line has very intensity. Based on the X-ray phase analysis was found, that change of solidification rate don't influence on the phases composition of investigated alloy. The X-ray phase analysis don't reveal occurring of Mg<sub>2</sub>Si and phases contains Mn and Al, what suggested that the fraction volume of these phases is below 3%.

SEM micrographs of MCMgAl3Zn1 cast after thermal analysis are shown in Figs. 9 and 10. Results from EDS analysis are shown in Table 4. EDS spectra for all samples confirms that, the matrix is  $\alpha$ -Mg, and intermetallics phases mostly likely Mg<sub>2</sub>Si, and Al-Mn (it could be a mixture of Al<sub>8</sub>Mn<sub>5</sub>, MnAl<sub>4</sub>). Because the size of particular elements of the structure is, in a prevailing measure, smaller than the diameter of the analyzing beam, the obtained at the quantitative analysis chemical composition may be averaged as a result of which some values of element concentrations may be overestimated.

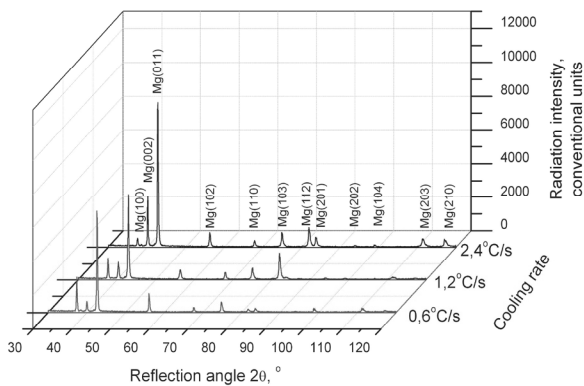


Fig. 8. XRD pattern of MC MgAl3Zn1 casting alloy at various solidification conditions

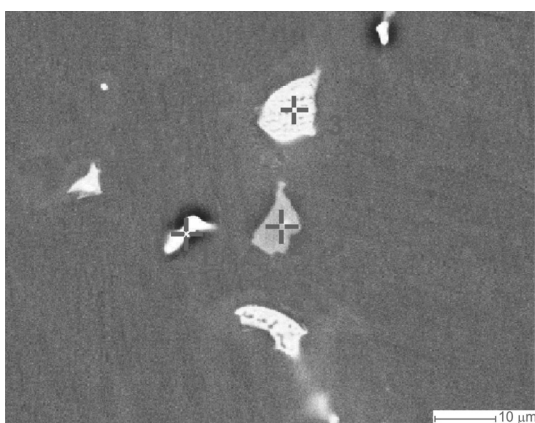


Fig. 9. Representative scanning electron microscope micrograph of magnesium alloy that solidified with cooling rate 2.4°C/s

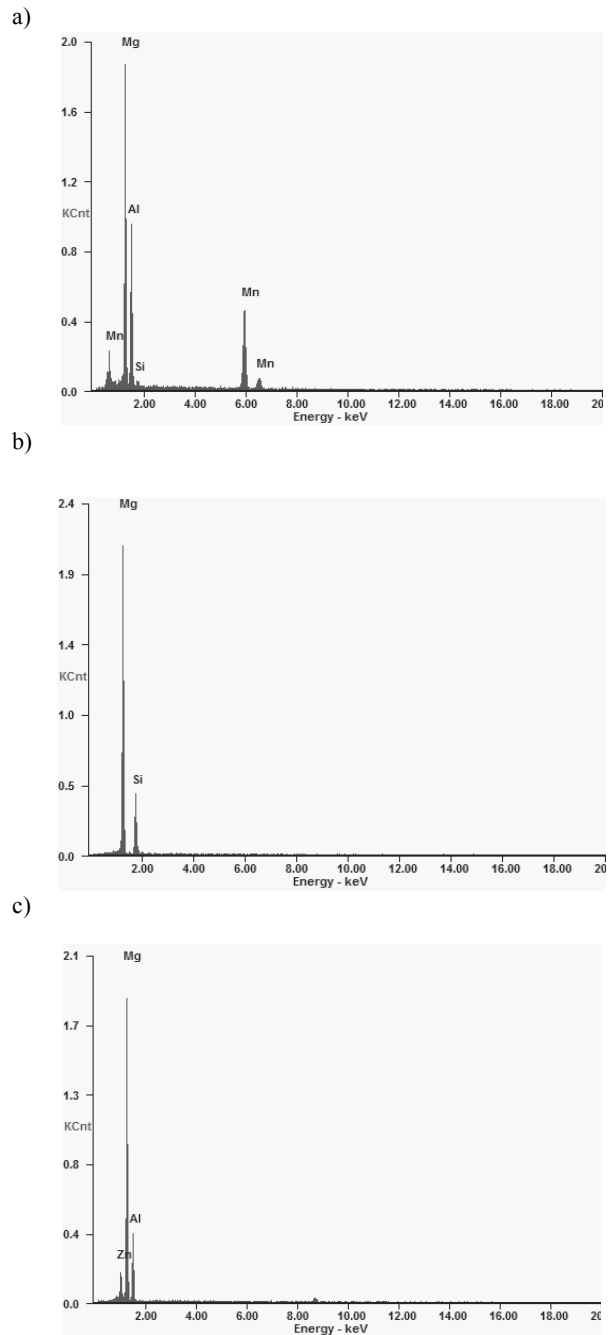


Fig. 10. Spectrum of the pointwise chemical composition analysis: a) point 1, b) point 2, c) point 3, from Fig 6

Figures 11 shows the solidification microstructures of MC Mg3Zn1 alloys at different cooling rates, which consisted of  $\alpha$ -Mg solid solution and Mg<sub>17</sub>Al<sub>12</sub> compound located in grain edge. The structure configurations at different experimental cooling rates were similar. The cooling rate had obvious effect on grain size of solidification microstructure. The grain size of magnesium alloy was determined by image

analysis, shows that the grain size decreases with increasing cooling rate.

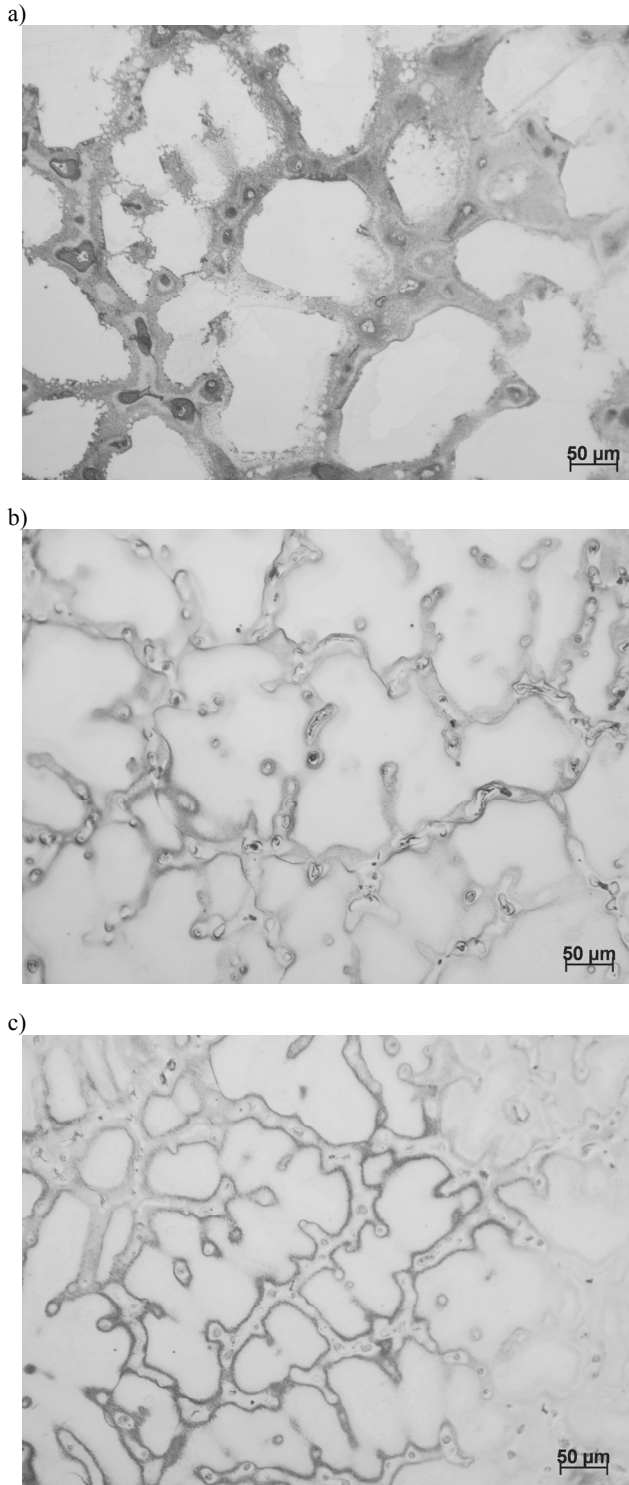


Fig. 11. Microstructures of MC MgAl<sub>3</sub>Zn<sub>1</sub> alloy solidified with cooling rate: a) 0.6°C/s, b) 1.2°C/s, c) 2.4°C/s. Magnification 100x

Table 4. Pointwise chemical composition analysis from Fig. 9

Analysis	Element	The mass concentration of main elements, %	
		weight	atomic
1	Mg	39.21	49.29
	Al	28.11	31.83
	Si	1.31	1.43
	Mn	31.37	17.45
2	Mg	70.20	73.13
	Si	29.8	26.87
3	Zn	9.48	3.86
	Mg	62.23	68.20
	Al	28.29	27.94

The grain size, Z, decreases from 179 to 85 μm with an increase of CR from 0.6 to 2.4°C/s.

### 3.3. Mechanical properties

Mechanical properties of the magnesium alloy are strongly dependent on the effect of grain size. Ultimate compressive strength increases with a decrease the grain size. Investigations results shows, the increase the cooling rate from 0.6°C/s to 2.4°C/s influence on the reduction of the grain size, what have influence on the ultimate compressive strength. The ultimate compressive strength increase from 245.94±3 MPa for lowest cooling rate to 275.78±3.01 MPa for highest cooling rate (Fig. 12).

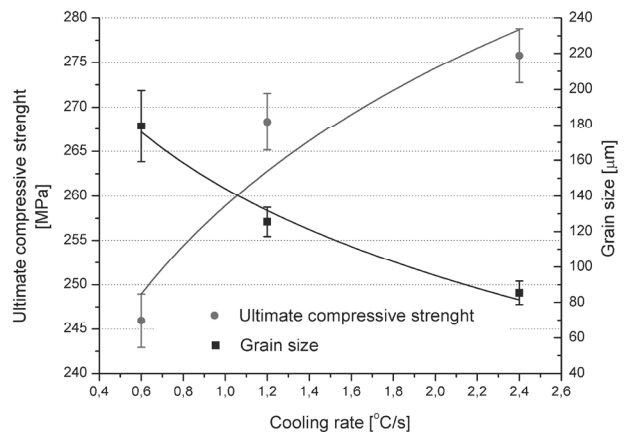


Fig. 12. Variation of the grain size and ultimate compressive strength as a function of cooling rate

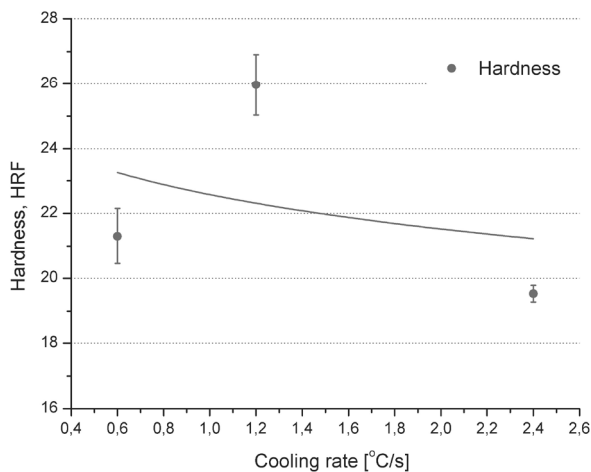


Fig. 13. Variation of the hardness as a function of cooling rate

Hardness of the magnesium alloys are strongly depended on the cooling rate. The hardness grows to value of 26 HRF with increment of the cooling rate to the 1.2°C/s. Further increment of cooling rate to 2.4°C/s causes decrement of hardness. It can be causes increase of microporosity.

## 4. Conclusions

The results are summarized as follows:

- Solidification parameters are affected by the cooling rate. The formation temperatures of  $T_N$  and  $T_{sol}$  are changed with an increasing cooling rate.
- As expected, the results show that grain size reduces as the cooling rate increases.
- Increasing the cooling rate increases significantly the Mg nucleate temperature, nucleation undercooling temperature and solidification range. These phenomena lead to an increased number of nucleus that affect the size of the grains.
- The X-ray phase analysis don't ravel occurring of  $Mg_2Si$  and phases contains Mn and Al, what suggested that the fraction volume of these phases is below 3%.
- Increasing the cooling rate increases the ultimate compressive strength.

## Acknowledgements

The authors would like to thank Dr. M. Kasprzak form the Silesian University of Technology in Poland for his valuable contributions to the UMSA Technology Platform's configuration.

## References

- [1] H. Zhang, S.B. Lin, L. Wu, J.C. Feng, Microstructural studies of friction stir welded AZ31 magnesium alloy, *Acta Metallurgica Sinica* 15/5 (2004) 747-753.
- [2] D. Kuc, E. Hadasik, G. Niewielski, A. Płachta, Structure and plasticity of the AZ31 magnesium alloy after hot deformation, *Journal of Achievements in Materials and Manufacturing Engineering* 27/1 (2008) 27-30.
- [3] H. Watari, T. Haga, Y. Shibue, K. Davey, N. Koga, Twin roll casting of magnesium alloys with high aluminum contents, *Journal of Achievements in Materials and Manufacturing Engineering* 18 (2006) 419-422.
- [4] K. Bryła, J. Dutkiewicz, P. Malczewski, Grain refinement in AZ31 alloy processed by equal channel angular pressing, *Archives of Materials Science and Engineering* 40/1 (2009) 17-22.
- [5] M. Greger, R. Kocich, L. Cížek, L.A. Dobrzański, I. Juička, Possibilities of mechanical properties and microstructure improvement of magnesium alloy, *Archives of Materials Science and Engineering* 28/2 (2007) 83-90.
- [6] K. Bryła, J. Dutkiewicz, M. Faryna, T.V. Dobatkina, L.L. Rokhlin, The influence of Nd and Ho addition on the microstructure of Mg-7Al alloy, *Archives of Materials Science and Engineering* 29/1 (2008) 40-44.
- [7] L.A. Dobrzański, T. Tański, L. Cížek, Heat treatment impact on the structure of die-cast magnesium alloys, *Journal of Achievements in Materials and Manufacturing Engineering* 20 (2007) 431-434.
- [8] G.T. Bae1, J.H. Bae1, D.H. Kang, H. Lee1, N.J. Kim, Effect of Ca addition on microstructure of twin-roll cast AZ31 Mg alloy, *Metals and Materials International* 15/1 (2009) 1-5.
- [9] M.M. Avedesian, H. Baker, *Magnesium and Magnesium Alloys 1999*: ASM International, Materials Park, USA.
- [10] I.J. Polmear, *Light Alloys*, London 1995.
- [11] C.J. Bettles, D.J. Rossouw, K. Venkatesan, *Magnesium alloys and Application*, New York, Wiley-VCH 2000.
- [12] E. Essadiqi, M.T. Shehata, A. Javaid, C. Galvani, G. Shen, S. Yue, R. Verma, Microstructure and temperature monitoring during the hot rolling of AZ31, *Journal of the Minerals, Metals and Materials Society* 61/8 (2009) 25-28.
- [13] S.S. Park, G.T. Bae, D.H. Kang, In-Ho Jung, K.S. Shind, N.J. Kimb, Microstructure and tensile properties of twin-roll cast Mg-Zn-Mn-Al alloys, *Scripta Materialia* 57 (2007) 793-796.
- [14] H. Watari, T. Haga, Y. Shibue, K. Davey, N. Koga, Twin roll casting of magnesium alloys with high aluminum contents, *Journal of Achievements in Materials and Manufacturing Engineering* 18 (2006) 419-422.
- [15] S.S. Park, W.J. Park, C.H. Kim, B.S. You N. J. Kim, The twin-roll casting of magnesium alloys, *Journal of the Minerals, Metals and Materials Society* 61/8 (2009) 14-18.
- [16] "Method and Apparatus for Universal Metallurgical Simulation and Analysis" - United States Patent, Patent No.: US 7,354,491 B2, Date of Patent: Apr. 8,2008.
- [17] S. Jura, Z. Jura, Theory of ATD method in researches of aluminium alloys. *Solidification of Metals and Alloys* 28 (1996) 57-87.